Carbohydrate Polymers 83 (2011) 375–382

Contents lists available at ScienceDirect

Carbohydrate Polymers

journal homepage: www.elsevier.com/locate/carbpol

Production and characterization of thick, thin and ultra-thin chitosan/PEO films

J. Li [a], S. Zivanovic [a,*], P.M. Davidson [a], K. Kit [b]

[a] Department of Food Science and Technology, University of Tennessee, 2605 River Drive, Knoxville, TN 37996, United States
[b] Department of Material Science and Engineering, University of Tennessee, Knoxville, TN 37996, United States

ARTICLE INFO

Article history:
Received 14 July 2010
Received in revised form 26 July 2010
Accepted 27 July 2010
Available online 6 August 2010

Keywords:
Chitosan
Polyethylene oxide
Blend films
Metal binding
Antibacterial efficacy

ABSTRACT

The current study focused on the functionality of chitosan/PEO films as affected by preparation methods, film composition, and thickness. Mixtures of chitosan and PEO with different blend ratios (100/0–50/50) were dissolved in 1% acetic acid to form 1% blend solutions. Films prepared by casting of 20 g or 10 g film-forming solution per 50-mm diameter polystyrene Petri dish or by using spin-coating method had an average thickness of 87.41 ± 5.44 μm (thick), 37.88 ± 2.41 μm (thin), and 70.47 ± 3.06 nm (ultra-thin), respectively. Development of polymer crystallization was monitored by X-ray diffractometer at ambient temperature; the metal-binding capacity of the films was assessed based on removal of chromium ions from K_2CrO_4 solution, and the antibacterial properties were tested against *Escherichia coli* K-12. The crystallization extent of the chitosan/PEO films decreased with decreased thickness as a consequence of faster solvent evaporation during film formation. Decreasing the thickness of the films increased the surface-to-mass ratio, what resulted in higher number of available active sites on the film surface per unit weight of chitosan, and promoted the metal-binding efficiency of the films. Ultra-thin chitosan/PEO films showed a significantly higher chromium-binding capacity [26.47–70.86 mg Cr(VI)/g film] compared to the cast films [0.73–7.59 mg Cr(VI)/g film]. However, these nano-thin films did not show significant antibacterial efficiency, most likely due to their extremely low weight and consequently insufficient chitosan concentration in the inoculated test tubes to kill significant number of bacteria.

1. Introduction

As a nontoxic, renewable and biodegradable polymer, chitosan has been extensively researched over the last two decades (Kumar, Muzzarelli, Muzzarelli, Sashiwa, & Domb, 2004). Due to the presence of amino and hydroxyl groups, chitosan exhibits multiple functionality including antimicrobial activity (Tsai & Su, 1999) and metal binding (Gamage & Shahidi, 2007). Many attempts have been conducted to develop functional materials from chitosan, such as films, sutures, beads, and hydrogels, and to apply them in the wound healing (Muzzarelli, 2009), drug delivery (Jin & Song, 2006; Kean & Thanou, 2010), metal removal (Selmer-Olsen et al., 1996), and antimicrobial food packaging (Ye, Neetoo, & Chen, 2008).

Blending of natural and synthetic polymers is a possibility for development of new materials such that the films formed by blending of two or more polymers commonly result in modified physical and mechanical properties compared to films made of the individual components. Our previous study showed that physical, mechanical, and antibacterial properties of films produced by blending chitosan and poly(ethylene oxide) (PEO) were altered—the chitosan fraction contributed to antimicrobial effect of the films, reduced tendency to spherulitic crystallization of PEO, and enhanced puncture and tensile strength of the films, while addition of the PEO resulted in thinner films with lower water vapor permeability (Zivanovic, Li, Davidson, & Kit, 2007).

Although chitosan films have significant metal-binding and antibacterial effects, these effects may be less expressed compared to efficiency of chitosan when in solutions (on equal chitosan weight basis) since chitosan molecules entrapped within the volume of the films are less assessable to bacterial cells and/or metal ions. In addition, possible crystallization of the polymer molecules during preparation and storage or application of the films could reduce the availability of active amino groups and thus reduce the film's efficiency. Increasing the surface-to-mass ratio of chitosan-based structures by making, e.g., nanofibers has been reported to result in superior functionalities (Desai, Kit, Li, & Zivanovic, 2008). Besides nanofibers, decreasing the thickness of the films to nanoscale is also a good way to increase the surface-to-mass ratio. Ultra-thin and modified chitosan films have been evaluated based on their physical and chemical properties (Ligler, Lingerfelt, Price, & Schoen, 2001; Nosal et al., 2005; Murray & Dutcher, 2006). Color change of cross-linked chitosan and poly(allyl amine) hydrochloride ultra-thin films upon metal binding has also been reported (Schauer et al., 2003). However, there is no available data on effects

* Corresponding author. Tel.: +1 865 974 0844; fax: +1 865 974 7332.
E-mail address: lanaz@utk.edu (S. Zivanovic).

0144-8617/$ – see front matter © 2010 Elsevier Ltd. All rights reserved.
doi:10.1016/j.carbpol.2010.07.064

of film thickness and chitosan/PEO bland ratio on physical and functional properties of the films. Thus, the objective of this study was to investigate effects of film thickness, composition and preparation methods on the film's performance.

2. Materials and methods

2.1. Film preparation

Low molecular weight chitosan (≤150 kDa) and high molecular weight PEO (900 kDa) were obtained from Aldrich Chemical Co. (Milwaukee, WI). Chitosan/PEO blend film-forming solutions (FFS) were prepared as 1% (w/w) of the mixture of chitosan and PEO with different ratio (100/0, 90/10, 80/20, 70/30, 60/40, 50/50) dissolved in 1% (w/w) acetic acid with stirring over night at room temperature. The FFS were filtrated through Miracloth® (Calbiochem-Novabiochem Corp., San Diego, CA) and centrifuged for 1 h at 15,500 rpm. Thick and thin chitosan/PEO films were prepared by pouring 20 g and 10 g FFS into 50-mm diameter Petri dishes and the solvent was evaporated in a vacuum oven at 38 °C under 17 kPa pressure for 48 and 24 h, respectively. The dried films were peeled from the Petri dishes and conditioned in desiccators at 25 °C and 20% RH prior to testing.

For preparation of ultra-thin chitosan/PEO films, the 4 cm^2 silicon chips were pre-cleaned by immersing in a solution of conc. H_2SO_4:30% H_2O_2 (3:1) for 1 h, followed by rinsing with d.i. water, and drying under a nitrogen stream. Ultra-thin chitosan/PEO films were prepared by placing 0.5 mL chitosan/PEO solutions on a silicon chip and spinning it using a spin coater (P-6708 D, Special Coating Systems Inc., Indianapolis, IN) at 2500 rpm for 60 s.

2.2. Film thickness

Thickness of the cast films was determined on 6 films per ratio treatment averaging measurements at 5 points for each film using a hand-held microcaliper (Mitutoyo Corp., Kawasaki, Kanagawa, Japan). Thickness of ultra-thin films was assessed on 4 films per ratio treatment averaging measurements at 5 points for each film using an ellipsometer (Gaertner Scientific Corp., Skokie, IL). The manually entered indexes of refraction for the chitosan and PEO were 1.50 and 1.45, respectively (Jiang et al., 1996).

2.3. Film crystallization

Film crystallization was monitored by X-ray diffractometry at ambient temperature. The crystallization of thick and thin films was conducted using a Molecular Metrology SAXD/WAXD system (Northampton, MA) equipped with a monochromic Cu Kα (1.5418 Å) X-ray source, a three-pin-hole alignment, and two-dimensional detector operating at 45 kV and 0.66 mA with the beam size of 30 μm. The WAXD patterns were recorded on reusable Fuji image plates, with the sample-to-film distance for 36.52 mm. The image plate was scanned in a Fuji X BAS-1800II image analyzer and the resultant image was converted to intensity vs. 2θ; or q plot using Polar X-ray analysis software. The data were collected over an angular range from 5° to 40° 2θ in a continuous mode. Relative crystallinity percentage (X_c) of the films were calculated by the following equation:

$$X_c\,(\%) = \left[\frac{A_c}{A_c + A_a}\right] \times 100$$

where A_c and A_a are the areas of the crystalline and amorphous regions, respectively.

The crystalline structure of polymers in the ultra-thin films was analyzed using grazing incidence X-ray diffraction (GID) method on a Philips X'Pert X-ray diffractometer (PANalytical B.V., The Netherlands) with a copper tube. The diffractograms were recorded with the tube operating at 45 kV and 40 mA with an X-ray incidence angle range between 5.025 and 39.975.

2.4. Ultra-thin film surface morphology

Atomic force microscopy (AFM) was used to study the surface roughness and morphology of ultra-thin chitosan/PEO films in air. AFM topographic images were obtained at room temperature using a multimode AFM with a Nanoscope III controller (Digital Instruments Veeco Metrology Group, Santa Barbra, CA) in tapping mode. The scan size was 1 μm^2 and the scan rate was 1.001 Hz with 512 pixels collected per line. The roughness of the surface was determined by measuring the root-mean-square (RMS) roughness parameter.

2.5. Film metal-binding capacity

Film metal-binding capacity of chitosan/PEO films was determined as change in concentration of Cr(VI) before and after adding films to test solution. Concentration of Cr(VI) in solutions was monitored following NIOSH method (NIOSH Manual of Analytical Methods (NMAM), 1994). Thick and thin films (one quarter of a film, ~4.9 cm^2) were soaked into 25 mL of 5 mg Cr(VI)/L of K_2CrO_4 solution and ultra-thin films (one silicon chip with film, ~4 cm^2) were soaked into 25 mL of 1 mg Cr(VI)/L of K_2CrO_4 solution. Both K_2CrO_4 solutions had pH of 7.3. All the samples were continuously shaken on a shaker for 3 h. Solutions of K_2CrO_4 with no films were equally treated and used as control. For ultra-thin films, K_2CrO_4 solutions with blank silicon chips were used as control. After 3 h of contact, 1 mL of sample solution was taken and mixed with 7 mL 0.5N H_2SO_4 in 25 mL volumetric flask, 0.5 mL sym-diphenylcarbazide solution in 50% acetone was added to the above solution as an indicator, and the volume was adjusted to 25 mL with 0.5N H_2SO_4. The absorbance of these solutions was measured at 540 nm using spectrophotometric method with 10-cm cuvette (UV-2102PC, Shimadzu, Kyoto, Japan). The chromium-binding capacity of chitosan/PEO films was calculated on film weight basis [mg chromium/g film], and on area basis [mg chromium/cm^2 film].

2.6. Antibacterial efficiency of the films

Antibacterial test was carried out by submerging thick and thin chitosan /PEO films (one quarter of a film, ~4.9 cm^2) and ultra-thin films (one silicon chip with film, ~4 cm^2) into culture tubes containing 10 mL sterile phosphate buffer (0.05 M, pH = 7.08) inoculated with ca. 10^6 CFU/mL *Escherichia coli* K-12. The tubes were vortexed and incubated for 6 h at 25 °C. The number of survived *E. coli* K-12 was determined using the pour plate method on trypticase soy agar (TSA) medium (Swanson, Petran, & Hanlin, 2001).

2.7. Statistical analysis

If not otherwise noted, the measurements were done in triplicate with individually prepared films as the replicated experimental units. Significant differences between groups were determined using Tukey–Kramer's HSD test in the JMP program (JMP, 2007). In all tables, means within the same group with a different letter are significantly different ($p < 0.05$).

Table 1
Thickness of thick, thin and ultra-thin chitosan/PEO blend films with weight ratio from 100/0 to 50/50[a].

Chitosan/PEO	Thick films (μm)	Thin films (μm)	Ultra-thin films (nm)
100/0	94.07 ± 10.70A	35.80 ± 0.60ab	72.33 ± 1.98a
90/10	92.93 ± 7.60A	41.47 ± 4.64a	69.40 ± 0.70b
80/20	89.07 ± 6.31A	38.20 ± 0.87ab	73.85 ± 0.37a
70/30	84.47 ± 1.42A	38.07 ± 2.12ab	72.95 ± 0.39a
60/40	83.13 ± 2.04A	39.07 ± 1.55ab	66.04 ± 1.31c
50/50	80.80 ± 4.66A	34.67 ± 0.76b	68.23 ± 1.33b

[a] Values reported are means and standard deviation. Different letters indicate the significant difference of data within the same column at $p < 0.05$ by Tukey–Kramer's HSD test (JMP, 2007).

3. Results and discussion

3.1. Film appearance and thickness

All cast chitosan/PEO films were transparent and the yellowish coloration from chitosan was reduced with increased PEO content, similarly to results reported by Alexeev, Kelberg, Evmenenko, and Bronnikov (2000). The mass of films produced from 20 g and 10 g FFS was 0.19–0.20 g and 0.09–0.10 g per film with surface area of 19.6 cm^2, respectively. The corresponding thickness was 80.80–94.07 μm for thick and 34.67–41.47 μm for thin films (Table 1). The ultra-thin chitosan/PEO films had thickness of 66.04–73.85 nm (Table 1). All ultra-thin films were of purple color and with no visible defects. However, the spinning caused accumulation of film-forming solution on the edges of the silicon wafers resulting in higher thickness and blue coloration. Fig. 1 demonstrates the appearance of 100/0 ultra-thin chitosan/PEO films as an example. The relationship between film reflection color and thickness was consistent with the results from Schauer et al. (2003), who reported that 110-nm thick chitosan–Resimene/TEG films reflected blue color. The mass of ultra-thin films was estimated at 0.025 mg/4 cm^2, based on weight changes of silicon chips before and after forming films on them. As suggested by Jiang et al. (1996), good adhesion was obtained when the substrates were processed under clean conditions. Ultra-thin films of all chitosan/PEO ratios had good adhesion when the silicon chips were cleaned as described.

With increase of PEO fraction in the blends, the thickness of cast films showed decreasing trend, while the thickness of ultra-thin chitosan/PEO films decreased significantly with increase of PEO content. This reduction may be explained by the contraction of the three-dimensional film matrixes due to strong intermolecular interactions between chitosan and PEO molecules (Pierro et al., 2007). In addition, lower viscosity of film-forming solution with addition of PEO may also contributed to thinner films (Affrossman, Kiff, O'Neill, Pethrick, & Richards, 1999), especially those formed by spin coating. In our situation, the increasing PEO content in the blends decreased the viscosity of solution from 0.21 Pa s for 100/0 chitosan/PEO solution to 0.12 Pa s for 50/50 chitosan/PEO solution.

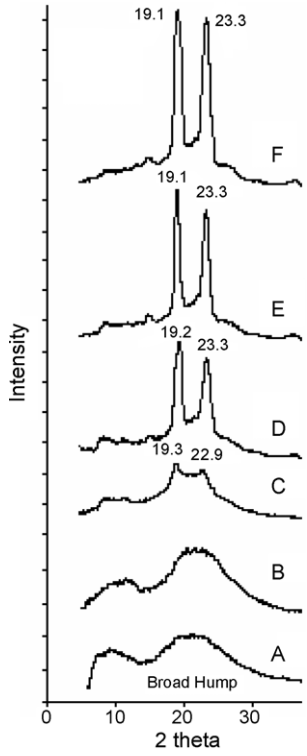

Fig. 2. 2θ-scan wide-angle X-ray diffraction (WAXD) spectra of thick films with chitosan/PEO blend ratio of (A) 100/0, (B) 90/10, (C) 80/20, (D) 70/30, (E) 60/40, and (F) 50/50.

3.2. Film crystallization

Wide-angle X-ray diffraction (WAXD) patterns and peaks at the corresponding diffraction angle (2θ) of thick films formed by solution casting are presented in Fig. 2 and relative crystallinity percentage values (X_c) of thick and thin films are listed in Table 2. The diffractograms of 100/0 and 90/10 films did not show characteristic peaks but rather a broad hump in the range of 10–40° 2θ, what indicated a predominantly amorphous form of the chitosan in the films (Fig. 2: A, B). In contrast, all of the diffraction patterns of 80/20–50/50 chitosan/PEO cast films had two sharp peaks with high intensity, resulting from PEO crystals (Fig. 2: C–F).

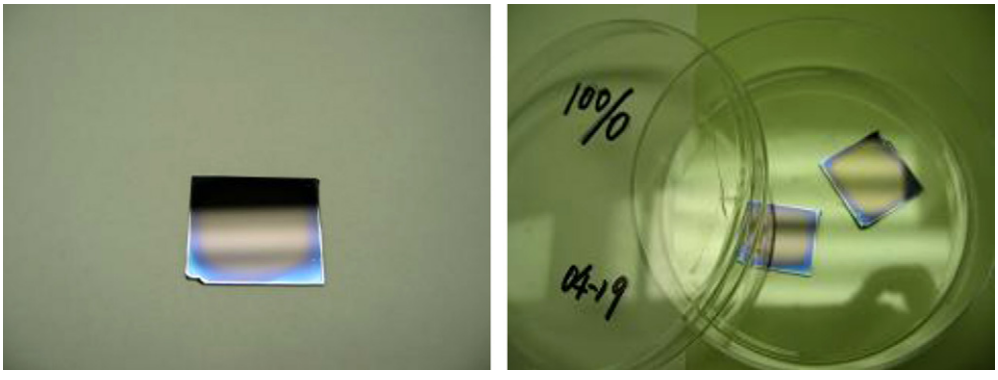

Fig. 1. Ultra-thin chitosan films prepared by placing 0.5 mL chitosan solutions on the silicon chips and spun using a spin coater at spin speed of 2500 rpm for 60 s.

Table 2
Relative crystallinity percentage (X_c) of the thick and thin chitosan/PEO blend films with weight ratio from 100/0 to 50/50.

Chitosan/PEO	Thick films	Thin films
100/0	a[a]	a
90/10	a	a
80/20	32.2%	14.9%
70/30	40.6%	28.7%
60/40	42.1%	36.7%
50/50	45.9%	34.3%

[a] There is no readable crystalline peak.

Contrary to chitosan powder with two main diffraction peaks due to its crystalline state, chitosan films generally exist in amorphous state with the two characteristic peaks of much smaller intensity. The amorphous state of chitosan in the films is a consequence of the inter- and intramolecular interactions between the amino and hydroxyl groups what limits the molecular movement of the chitosan chains and prevents its crystallization (Fuentes, Retuert, Ubilla, Fernandez, & Gonzalez, 2000; Nunthanid, Puttipipatkhachorn, Yamamoto, & Peck, 2001). PEO is a semi-crystalline polymer that easily forms spherulic crystals from solutions (Mucha, Piekielna, & Wieczorek, 1999). The position of two major peaks in the diffractograms of the blend samples were always at 19.0° and 23.3° 2θ (Fig. 2), what is similar to results from Huang and Chen (2001), indicating unit-cell structures of the PEO crystals. Chitosan content in the blend limited extent of the PEO crystal formation. However, no significant shift in the diffraction peaks was observed, indicating that the presence of chitosan did not affect the ordered structure of PEO but only limited the nucleation process (Mucha et al., 1999; Peesan, Supaphol, & Rujiravanit, 2005). Similarly, chitosan has been reported to retard the crystallinity of films made of cellulose (Isogai & Atalla, 1992), poly(3-hydroxybutyric acid) (Ikejima & Inoue, 2000), nylon 11 (Kuo, Sahu, & Yu, 2006), polycaprolactone (Sarasam, Krishnaswamy, & Madihally, 2006), and poly(vinyl alcohol) (Chen, Wang, Mao, & Yang, 2007). This may be explained by that the chitosan molecular chains affected the overall mobility of polymers in the blend and impeded the rate of crystal growth (Zhao, Yu, Zhong, Zhang, & Sun, 1995).

According to data presented in Table 2, crystallinity of the thick films was generally higher than of the thin films when films of the same blend ratios were compared. For the films with blend ratios 50/50–80/20, the corresponding values of X_c were 32.2–45.9% for thick films and 14.9–34.3% for thin films (Table 2). One possible reason for higher crystallinity in thicker films is the longer drying time what prolonged movement of polymer chains, allowed their assembly and, finally, formation of more PEO crystals. On the other hand, no crystal peaks were detected in ultra-thin chitosan/PEO films except a very small diffraction peak in 50/50 films (Fig. 3). The X-ray diffraction data clearly show that spin-coating method greatly reduced the crystallization extent of chitosan and PEO in the films. The rapid solvent evaporation during formation of ultra-thin films caused the sudden onset of restricted mobility of the polymer chains and froze-in the phase structures, resulting in a minimum extent of crystallization in films (Affrossman et al., 1999). Similar results were reported by Jiang et al. (1996) who noted that chitosan nano-thin films with the thickness of 300 nm had amorphous structure.

3.3. Ultra-thin film surface morphology

Tapping mode atomic force microscopy (AFM) was used to evaluate the surface morphology of nano-thin chitosan/PEO films (Fig. 4). Pure PEO ultra-thin films were also investigated for the comparison. As observed from Fig. 4A and E, the surface morphology of pure chitosan films was uniform and smooth whereas the pure PEO films were considerable rough, suggesting that PEO molecules crystallized regardless to rapid evaporation of the solvent during spinning. As the PEO content in the blend increased, the surface topology began to alter. The 3D images clearly illustrate increasing the number and height of the peaks on the films surface with increased PEO fraction (Fig. 4B–D). Table 3 gives the RMS of roughness values for corresponding ultra-thin films. The pure chitosan ultra-thin films had RMS roughness of 0.377 nm, which was consistent with the results from Nosal et al. (2005), whereas the RMS roughness of the blend ultra-thin films increased from 1.110 nm for 90/10 chitosan/PEO films to 2.047 nm for 50/50 chitosan/PEO films. Replacing even 10% of chitosan with PEO significantly increased the surface roughness of the ultra-thin films.

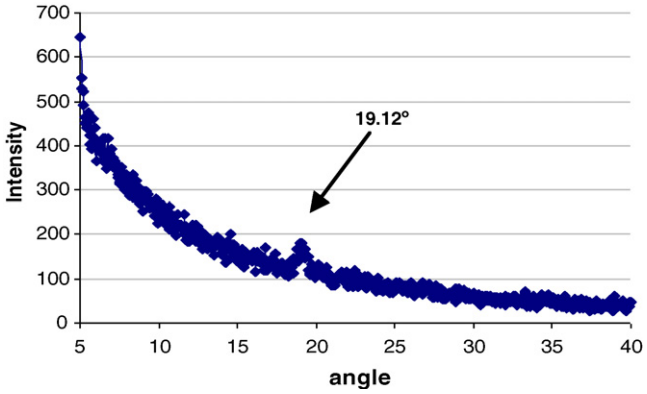

Fig. 3. X-ray diffractogram of grazing incidence pattern on 50/50 ultra-thin chitosan /PEO films.

Table 3
The root-mean-square (RMS) of roughness values for surfaces of ultra-thin chitosan/PEO films with blend ratios of 100/0, 90/10, 80/20, 50/50 and 0/100.

Chitosan/PEO	RMS roughness (nm)
100/0	0.377
90/10	1.110
80/20	1.564
50/50	2.047
0/100	2.660

3.4. Film metal-binding capacity

Pure chitosan and 90/10 chitosan/PEO thick and thin films completely dissolved in chromium solutions and their chromium-binding capacity could not be determined. Chitosan/PEO thick films with blend ratio 80/20–50/50 bound 25.8–95.9% of Cr(VI) from 25 mL 5 mg Cr(VI)/L while thin films of the same composition bound 23.8–96.7% under same conditions. These results indicate no significant difference in amount of removed chromium ions although the thin films were of about half weight of thick films used in this test (0.09–0.10 g/film vs. 0.19–0.20 g/film). With estimated film weight of only 0.025 mg, ultra-thin chitosan/PEO films still bound 8.1–11.9% of chromium ions from the test solution.

When results are expressed based on amount of chromium ions bound by 1 cm^2 film, the cast films performed similarly, 3.42–12.21 $\times 10^{-3}$ mg Cr/cm^2 and 3.04–12.32 $\times 10^{-3}$ mg Cr/cm^2 for thick and thin films, respectively; ultra-thin films with the same surface area bound only 0.17–0.44 $\times 10^{-3}$ mg Cr/cm^2 (Table 4). However, when results are expressed based on amount of chromium bound by 1 g of the film, the ultra-thin chitosan/PEO films had significantly higher binding capacity (26.47–70.86 mg Cr/g film) compared to the cast thick (0.73–2.86 mg Cr/g film) and thin films (1.04–6.21 mg Cr/g film)

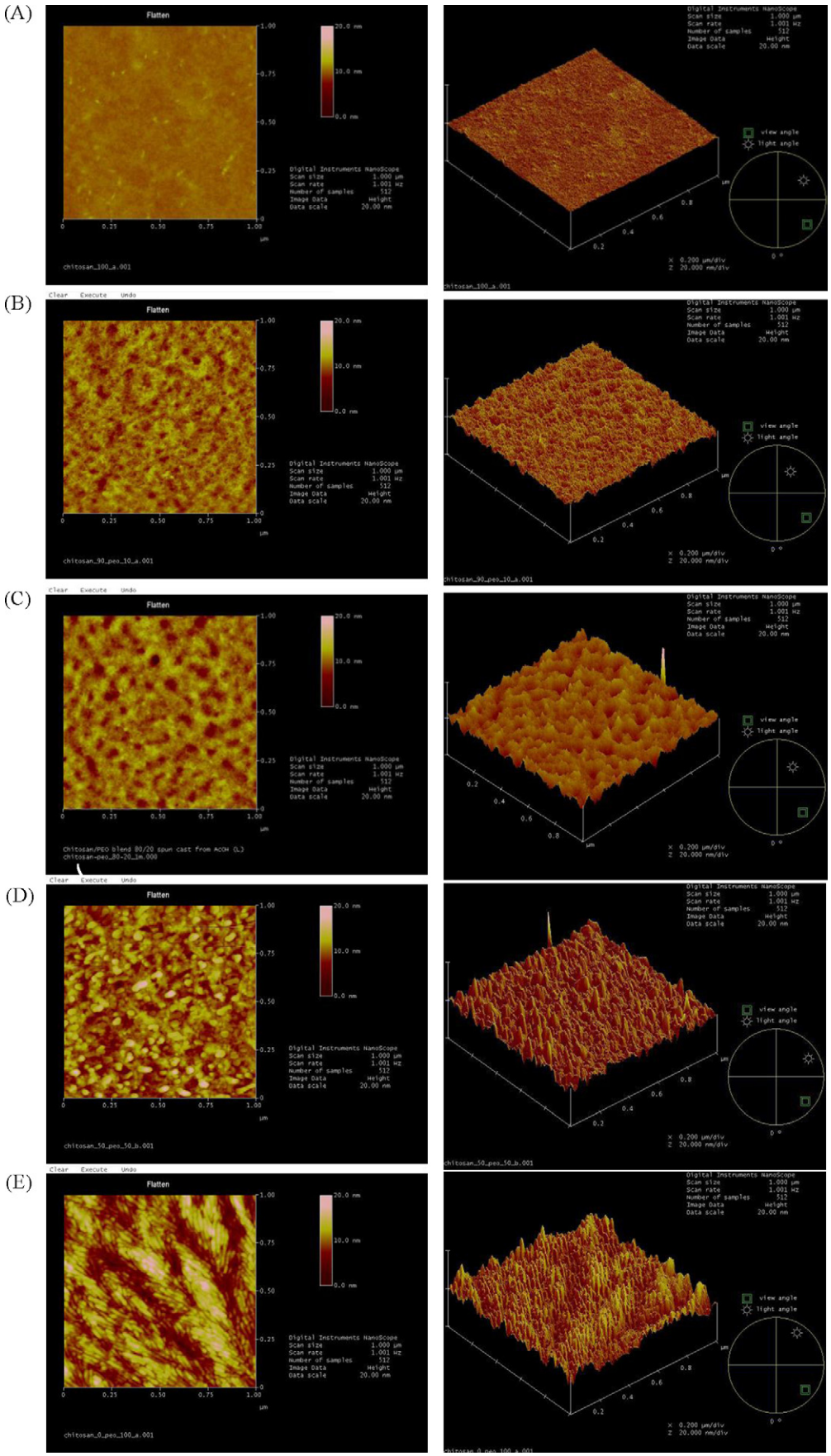

Fig. 4. Tapping mode AFM two and three-dimensional images of 1 μm scans for ultra-thin chitosan/PEO blending films with ratios of (A) 100/0, (B) 90/10, (C) 80/20, (D) 50/50, and (E) 0/100.

Table 4
Cr(VI) binding capacities of thick, thin and ultra-thin chitosan/PEO films[a].

Chit/PEO	mg Cr(VI) bound by 1 g film			10^{-3} mg Cr(VI) bound by 1 cm^2 film		
	Thick films	Thin films	Ultra-thin films	Thick films (both sides)	Thin films (both sides)	Ultra-thin films (one side)
100/0	–	–	32.82 ± 14.19A	–	–	0.21 ± 0.09A
90/10	–	–	40.24 ± 24.00A	–	–	0.25 ± 0.15A
80/20	0.73 ± 0.19b	1.04 ± 0.08c	26.47 ± 0.53A	3.42 ± 0.43d	3.04 ± 0.30c	0.17 ± 0.01A
70/30	1.67 ± 0.10ab	2.51 ± 0.91bc	70.86 ± 20.39A	6.54 ± 0.28c	6.07 ± 1.05b	0.44 ± 0.13A
60/40	2.25 ± 0.90ab	7.59 ± 1.51ab	59.10 ± 12.47A	9.12 ± 0.71b	10.89 ± 0.07a	0.37 ± 0.08A
50/50	2.86 ± 0.17a	6.21 ± 0.98a	36.65 ± 17.32A	12.21 ± 0.04a	12.32 ± 0.01a	0.23 ± 0.11A

[a] Values reported are means and standard deviation. Different letters indicate the significant difference of data within the same column at $p < 0.05$ by Tukey–Kramer's HSD test (JMP, 2007).

(Table 4). Metal binding occurs due to the electrostatic attraction between the dissociated CrO_4^{2-} ions in solution and NH_3^+ group of chitosan (Qian, Huang, Jiang, He, & Wang, 2000). The metal-binding capacity of chitosan films varies with type of metal ions, extent of film crystallinity, pH value of the solution, number of available amino groups, and physical adsorptive ability of the films (Kurita, Sannan, & Iwakura, 1979; Modrzejewska & Kaminski, 1999). Apparently, films with larger surface area per weight have more amino groups available to interact with chromium ions and consequently remove more metal ions from solution. In our study, the surface-to-mass ratio of thick, thin, and ultra-thin films was 0.017–0.026 m^2/g, 0.036–0.058 m^2/g, and 16 m^2/g, respectively what explains superior performance of ultra-thin films when expressed as amount of chromate ions bound per unit weight of the films. However, if binding of metal ions by the films occurs exclusively on the surface of the films, than all three types of the films should bind similar amount of chromate ions per 1 cm^2 but we noticed more than 10-fold difference between cast and spun films. Consequently, diffusion of solvent (water) and metal ions (CrO_4^{2-}) into the volume of the films should be taken in account in attempt to determine true efficiency of the films. If we consider an average thickness for thick films to be 90 μm, for thin films 40 μm, and for ultra-thin films 70 nm (round values based on Table 1), than thick films were more than 1200, and thin films more than 400 times thicker than ultra-thin films. If we assume that whole volume/depth of 70-nm films was saturated with the chromium solution (chromate ion diffused through the whole volume of the films), the question is what would be the maximum depth to which the chromate ions may diffuse into chitosan films during the metal-binding test (while the films was submerged into the solution). If we further assume that there is no gradient in concentration of chromate ions throughout the part of the film in which CrO_4^{2-} diffused, we can calculate that if 1 cm^2 of 70-nm film binds 0.17 μg Cr/cm^2 (80/20, Table 4 with exact thickness of 73.85 nm, Table 1) and 1 cm^2 of 40-μm film (38.2 μm exactly) binds 3.04 μg Cr/cm^2, the depth of diffusion of chromate ions into thin film was 0.660 μm on each side (~9 times more than in ultra-thin films where diffusion depth was limited simply by thickness of the film). These 1.32 μm was 3.46% of the total thickness of the thin 80/20 film or in other words, only approx. 3.5% of the film's volume was efficient in metal binding ('efficient fraction'). Overall percentage of film depth to which chromium diffused in thick films was lower than into thin films (Table 5). Currently, we are conducting studies to determine depth of chromium diffusion in chitosan films as affected by time and film composition.

Table 5
Calculated depth of diffusion of Cr(VI) in thick and thin films based on results for ultra-thin chitosan/PEO films.

Chitosan/PEO	Depth of diffusion on each side of film (μm)			% thickness of film in which chromate diffused		
	Thick	Thin	Ultra-thin[a]	Thick	Thin	Ultra-thin
80/20	0.743	0.660	0.074	1.67	3.46	(100)
70/30	0.542	0.503	0.073	1.28	2.64	(100)
60/40	0.814	0.972	0.066	1.96	4.97	(100)
50/50	1.811	1.827	0.068	4.48	10.54	(100)

[a] Measured thickness of ultra-thin films.

Although our results were lower compared to chemically modified cross-linked xanthated chitosan flakes and beads with adsorption capacities of 625 mg/g and 256 mg/g, respectively (Sankararamakrishnan, Dixit, Iyengar, & Sanghi, 2006), they were higher than those obtained for plain chitosan powder with 27.3 mg/g (Udaybhaskar, Iyengar, & Prabhakararao, 1990) and high molecular weight chitosan/PEO nanofibers with 3–17 mg/g chitosan (Desai et al., 2008). Interestingly, replacement of up to 50% of chitosan with PEO did not significantly reduce the metal-binding capacity of the cast films. On the contrary, there was an increasing tendency in metal binding with increase of PEO content. This may be explained by the extent of diffusion of CrO_4^{2-} into the films. The intermolecular interactions between chitosan and PEO molecules impeded the high packing density of polymers within the film and contributed to their binding of heavy metal ions (Liu & Bai, 2006). There was no significant difference in performance of chromium bound by ultra-thin chitosan/PEO films with different blend ratio due to their extremely low weight and low adsorptive ability.

Table 6
Inhibitory effects of thick and thin chitosan/PEO films toward *E. coli* K-12 inoculated in sterile phosphate buffer (0.05 M, pH = 7.08) and stored for 6 h at 25 °C[a].

Chit/PEO	Thick films			Thin films		
	Weight (g)	Concentration of chitosan in inoculated test tubes (%)	*E. coli* K-12 reduction (log 10 CFU/mL)	Weight(g)	Concentration of chitosan in inoculated test tubes (%)	*E. coli* K-12 reduction (log 10 CFU/mL)
100/0	0.047	0.470	2.67 ± 0.05ab	0.023	0.230	2.37 ± 0.08abc
90/10	0.058	0.522	3.11 ± 0.21a	0.026	0.235	2.20 ± 0.15bc
80/20	0.055	0.440	2.90 ± 0.10ab	0.025	0.200	2.40 ± 0.45abc
70/30	0.044	0.308	2.75 ± 0.07ab	0.021	0.147	2.56 ± 0.01abc
60/40	0.038	0.228	2.68 ± 0.29ab	0.027	0.162	2.62 ± 0.12abc
50/50	0.047	0.235	2.51 ± 0.16abc	0.017	0.085	1.80 ± 0.10c

[a] Means of three replicates ± standard deviation. Different letters indicate the significant difference of data within the same column at $p < 0.05$ by Tukey–Kramer's HSD test (JMP, 2007).

3.5. Antibacterial efficiency

The inhibitory effects of regular thick and thin chitosan/PEO films toward *E. coli* K-12 are shown in Table 6. The tested films had the similar surface area of 9.8 cm^2 (including two sides) but different mass, 0.038–0.058 g for thick and 0.017–0.027 g for thin films. As shown in Table 6, the thick chitosan/PEO films reduced the number of *E. coli* K-12 for 2.51–3.11 log CFU/mL, whereas the thin chitosan/PEO films reduced it for 1.80–2.62 log CFU/mL. The antibacterial efficiency of our cast films was similar to those found in the literature; Park, Daeschel, and Zhao (2004) have reported that 0.03 g chitosan films (average thickness 70 μm, surface area of 6.28 cm^2) reduced *E. coli* for 1.8 log CFU/g. Our results further indicate that antibacterial efficiency of the films was not significantly reduced by addition of up to 40% or 50% PEO, in thin and thick films, respectively.

Many studies have reported the inhibitory effect of chitosan against *E. coli* (Tsai & Su, 1999). One general consideration of the mechanism was the cationic amino groups $-NH_3^+$ on chitosan chains could interact with negative charged cell surface and change membrane permeability, causing the leakage of intracellular components and final death of cells (Tsai & Su, 1999). However, it appears that for this mechanism, chitosan molecules have to be dissolved rather than attached to matrix of a film. If chitosan has strong antimicrobial efficiency even on contact, its efficiency would be related to surface-to-mass ratio, similar to metal-binding behavior. In other words, under conditions of the same blend ratio, it would be expected that thinner films have same or better antibacterial ability than thick films. Based on our results, there were no significant differences in antimicrobial efficiency between the cast films of same bland ratio (Table 6). Furthermore, ultra-thin films did not show measurable efficiency against *E. coli*. Based on the method used to assess antimicrobial efficiency of the films, the reason for these results is probably in minute mass of chitosan spin-coated films resulting in extremely low concentration of chitosan (0.00025%) in the inoculated test tubes. Thus, it seems that chitosan-based films may exhibit antimicrobial properties only if there is sufficient fraction of chitosan fully dissolved.

4. Conclusions

The surface morphology, antimicrobial activity and metal-binding capacity of the chitosan/PEO films were affected by their composition and preparation methods. The incorporation of PEO in the chitosan films decreased the film thickness regardless on the preparation method. For the films with the same chitosan/PEO ratio, crystallinity was greater in thick than in thin films, while it was negligible in ultra-thin films indicating that the faster solvent evaporation, especially under spin-coating conditions, can greatly restrict the mobility of the polymer chains and prevent crystallization. The addition of up to 40% and 50% PEO in thin and thick chitosan films, respectively, did not significantly reduce chromium-binding capacity and antibacterial efficiency of the films, indicating that PEO could reduce the amount of chitosan with no effect on the functional properties of the films. Although ultra-thin chitosan/PEO films showed significantly higher chromium-binding capacity compared to the regular cast films, they did not show significant antibacterial properties because extremely low amount of chitosan per unit area. Chitosan/PEO films have potential to be used as functional packaging material in the food, agricultural, and pharmaceutical industries. In particularly, ultra-thin chitosan/PEO films show their high metal-binding effectiveness and have potential to be used as coatings, sensors, or layers incorporated into packaging.

Acknowledgments

This research was funded by U.S. EPA Science To Achieve Results (STAR) program grant #GR832372 and Hatch fund from the Tennessee Experiment Station TEN264.

References

Affrossman, S., Kiff, T., O'Neill, S. A., Pethrick, R. A., & Richards, R. W. (1999). Topography and surface composition of thin films of blends of poly(methyl methacrylate) and poly(ethylene oxide). *Macromolecules*, *32*, 2721–2730.

Alexeev, V. L., Kelberg, E. A., Evmenenko, G. A., & Bronnikov, S. V. (2000). Improvement of the mechanical properties of chitosan films by the addition of poly(ethylene oxide). *Polymer Engineering and Science*, *40*(5), 1211–1215.

Chen, C., Wang, F., Mao, C., & Yang, C. (2007). Studies of chitosan. I. Preparation and characterization of chitosan/poly(vinyl alcohol) blend films. *Journal of Applied Polymer Science*, *105*, 1086–1092.

Desai, K., Kit, K., Li, J., & Zivanovic, S. (2008). Morphological and surface properties of electrospun chitosan nanofibers. *Biomacromolecules*, *9*, 1000–1006.

Fuentes, S., Retuert, P. J., Ubilla, A., Fernandez, J., & Gonzalez, G. (2000). Relationship between composition and structure in chitosan-based hybrid films. *Biomacromolecules*, *1*, 239–243.

Gamage, A., & Shahidi, F. (2007). Use of chitosan for the removal of metal ion contaminants and proteins from water. *Food Chemistry*, *104*, 989–996.

Huang, C., & Chen, J. (2001). Crystallization and chain conformation of semicrystalline and amorphous polymer blends studied by wide-angle and small-angle scattering. *Journal of Polymer Science Part B-Polymer Physics*, *39*, 2705–2715.

Ikejima, T., & Inoue, Y. (2000). Crystallization behavior and environmental biodegradability of the blend films of poly(3-hydroxybutyric acid) with chitin and chitosan. *Carbohydrate Polymers*, *41*, 351–356.

Isogai, A., & Atalla, R. H. (1992). Preparation of cellulose–chitosan polymer blends. *Carbohydrate Polymers*, *19*, 25–28.

Jiang, H., Su, W., Caracci, S., Bunning, T. J., Cooper, T., & Adams, W. W. (1996). Optical waveguiding and morphology of chitosan thin films. *Journal of Applied Polymer Science*, *61*, 1163–1171.

Jin, J., & Song, M. (2006). Chitosan and chitosan–PEO blend membranes crosslinked by genipin for drug release. *Journal of Applied Polymer Science*, *102*, 436–444.

Kean, T., & Thanou, M. (2010). Biodegradation, biodistribution and toxicity of chitosan. *Advanced Drug Delivery Reviews*, *62*(1), 3–11.

Kumar, M. N. V. R., Muzzarelli, R. A. A., Muzzarelli, C., Sashiwa, H., & Domb, A. J. (2004). Chitosan chemistry and pharmaceutical perspectives. *Chemical Reviews*, *104*, 6017–6084.

Kuo, P., Sahu, D., & Yu, H. H. (2006). Properties and biodegradability of chitosan/nylon 11 blending films. *Polymer Degradation and Stability*, *91*, 3097–3102.

Kurita, K., Sannan, T., & Iwakura, Y. (1979). Studies on chitin. VI. Binding of metal cations. *Journal of Applied Polymer Science*, *23*, 511–515.

Ligler, F. S., Lingerfelt, B. M., Price, R. P., & Schoen, P. E. (2001). Development of uniform chitosan thin-film layers on silicon chips. *Langmuir*, *17*, 5082–5084.

Liu, C., & Bai, R. (2006). Adsorptive removal of copper ions with highly porous chitosan/cellulose acetate blend hollow fiber membranes. *Journal of Membrane Science*, *284*, 313–322.

Modrzejewska, Z., & Kaminski, W. (1999). Separation of Cr(VI) on chitosan membranes. *Industrial & Engineering Chemistry Research*, *38*, 4946–4950.

Mucha, M., Piekielna, J., & Wieczorek, A. (1999). Characterization and morphology of biodegradable chitosan/synthetic polymer blends. *Macromolecular Symposia*, *144*, 391–412.

Murray, C. A., & Dutcher, J. R. (2006). Effect of changes in relative humidity and temperature on ultrathin chitosan films. *Biomacromolecules*, *7*, 3460–3465.

Muzzarelli, R. A. A. (2009). Chitins and chitosans for the repair of wounded skin, nerve, cartilage and bone. *Carbohydrate Polymers*, *76*, 167–182.

NIOSH. (1994). *Manual of analytical methods (NMAM) 7600* (4th ed.). U.S. Department of Health and Human Services. Publ. (NIOSH)., pp. 94–113.

Nosal, W. H., Thompson, D. W., Yan, L., Sarkar, S., Subramanian, A., & Woollam, J. A. (2005). Infrared optical properties and AFM of spin-cast chitosan films chemically modified with 1,2 epoxy-3-phynoxy-propane. *Colloids and Surfaces B*, *46*, 26–31.

Nunthanid, J., Puttipipatkhachorn, S., Yamamoto, K., & Peck, G. E. (2001). Physical properties and molecular behavior of chitosan films. *Drug Development and Industrial Pharmacy*, *27*(2), 143–157.

Park, S. I., Daeschel, M. A., & Zhao, Y. (2004). Functional properties of antimicrobial lysozyme–chitosan composite films. *Journal of Food Science*, *69*(8), M215–221.

Peesan, M., Supaphol, P., & Rujiravanit, R. (2005). Preparation and characterization of hexanoyl chitosan/polylactide blend films. *Carbohydrate Polymers*, *60*, 343–350.

Pierro, P. D., Chico, B., Villalonga, R., Mariniello, L., Masi, P., & Porta, R. (2007). Transglutaminase-catalyzed preparation of chitosan–ovalbumin films. *Enzyme and Microbial Technology*, *40*, 437–441.

Qian, S. H., Huang, G. Q., Jiang, J. S., He, F., & Wang, Y. T. (2000). Studies of adsorption behavior of crosslinked chitosan for Cr(VI), Se(VI). *Journal of Applied Polymer Science*, *77*, 3216–3219.

Sankararamakrishnan, N., Dixit, A., Iyengar, L., & Sanghi, R. (2006). Removal of hexavalent chromium using a novel cross linked xanthated chitosan. *Bioresource Technology*, *97*, 2377–2382.

Sarasam, A. R., Krishnaswamy, R. K., & Madihally, S. V. (2006). Blending chitosan with polycaprolactone: effects on physicochemical and antibacterial properties. *Biomacromolecules*, *7*, 1131–1138.

Schauer, C. L., Chen, M., Chatterley, M., Eisemann, K., Welsh, E. R., Price, R. R., et al. (2003). Color changes in chitosan and poly(allyl amine) films upon metal binding. *Thin Solid Films*, *434*, 250–257.

Selmer-Olsen, E., Ratnaweera, H. C., & Pehrson, R. R. (1996). A novel treatment process for dairy wastewater with chitosan produced from shrimp-shell waste. *Water Science and Technology*, *34*(11), 33–40.

Swanson, K. M. J., Petran, R. L., & Hanlin, J. H. (2001). *Culture methods for enumeration of microorganisms*. American Public Health Association, Washington, DC.

Tsai, G. J., & Su, W. H. (1999). Antibacterial activity of shrimp chitosan against *Escherichia coli*. *Journal of Food Protection*, *62*(3), 239–243.

Udaybhaskar, P., Iyengar, L., & Prabhakararao, A. V. S. (1990). Hexavalent chromium interaction with chitosan. *Journal of Applied Polymer Science*, *39*, 739–747.

Ye, M., Neetoo, H., & Chen, H. (2008). Control of *Listeria monocytogenes* on ham steaks by antimicrobials incorporated into chitosan-coated plastic films. *Food Microbiology*, *25*, 260–268.

Zhao, W., Yu, L., Zhong, X., Zhang, Y., & Sun, J. (1995). The compatibility and morphology of chitosan–poly(ethylene oxide) blends. *Journal of Macromolecular Science: Physics*, *B34*(3), 231–237.

Zivanovic, S., Li, J., Davidson, P. M., & Kit, K. (2007). Physical, mechanical and antibacterial properties of chitosan/PEO blend films. *Biomacromolecules*, *8*(5), 1505–1510.